JES

JOURNAL OF ENVIRONMENTAL SCIENCES

ISSN 1001-0742
CN 11-2629/X

July 1, 2013 Volume 25 Number 7
www.jesc.ac.cn

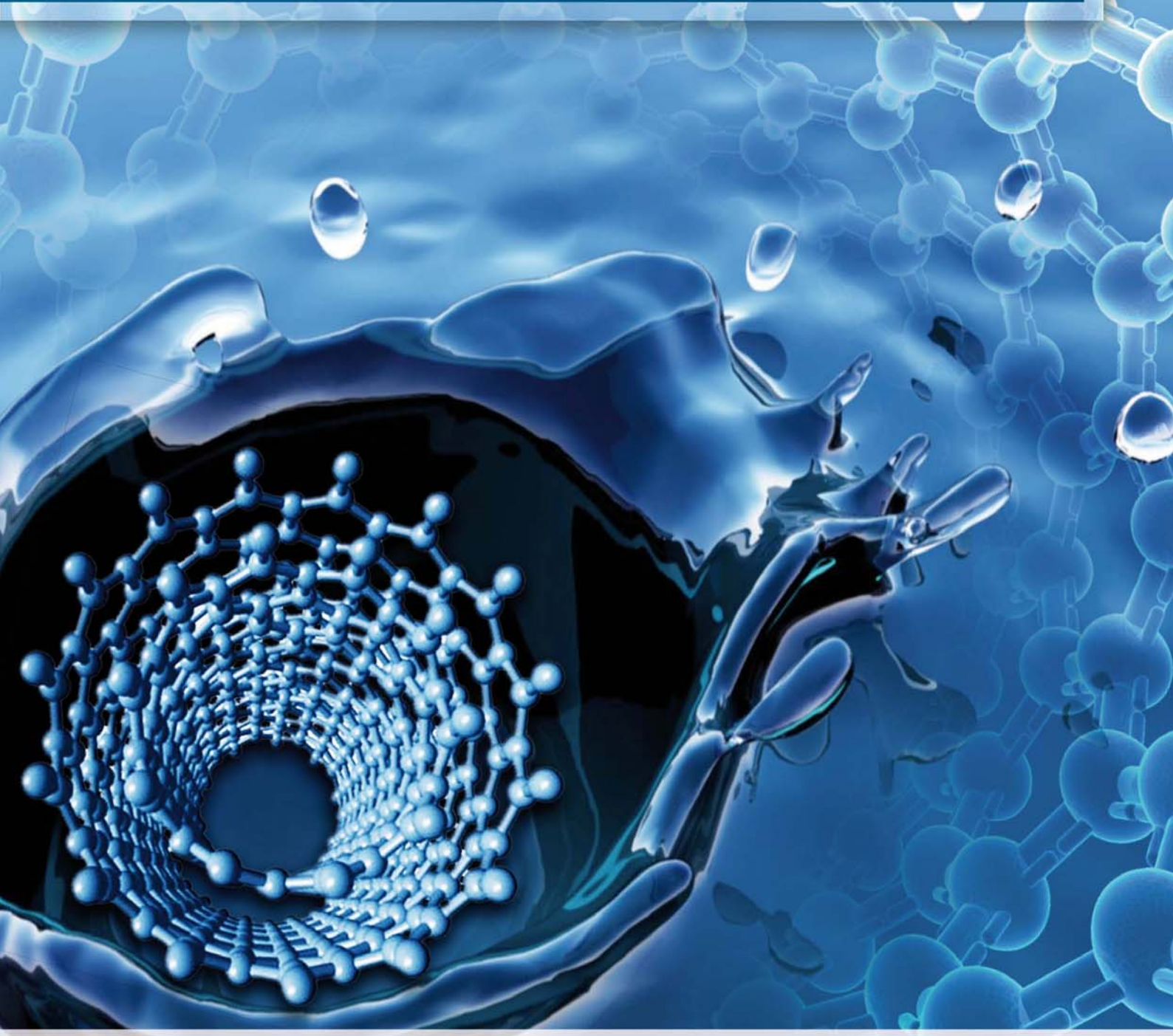

ELSEVIER

Science Press

Sponsored by
Research Center for Eco-Environmental Sciences
Chinese Academy of Sciences

ISSN 1001–0742 **Journal of Environmental Sciences** Vol. 25 No. 7 2013

CONTENTS

Aquatic environment

Application potential of carbon nanotubes in water treatment: A review
Xitong Liu, Mengshu Wang, Shujuan Zhang, Bingcai Pan ····· 1263

Characterization, treatment and releases of PBDEs and PAHs in a typical municipal sewage treatment plant situated beside an urban river, East China
Xiaowei Wang, Beidou Xi, Shouliang Huo, Wenjun Sun, Hongwei Pan, Jingtian Zhang, Yuqing Ren, Hongliang Liu ····· 1281

Factors influencing antibiotics adsorption onto engineered adsorbents
Mingfang Xia, Aimin Li, Zhaolian Zhu, Qin Zhou, Weiben Yang ····· 1291

Assessment of heavy metal enrichment and its human impact in lacustrine sediments from four lakes in the mid-low reaches of the Yangtze River, China
Haijian Bing, Yanhong Wu, Enfeng Liu, Xiangdong Yang ····· 1300

Biodegradation of 2-methylquinoline by *Enterobacter aerogenes* TJ-D isolated from activated sludge
Lin Wang, Yongmei Li, Jingyuan Duan ····· 1310

Inactivation, reactivation and regrowth of indigenous bacteria in reclaimed water after chlorine disinfection of a municipal wastewater treatment plant
Dan Li, Siyu Zeng, April Z. Gu, Miao He, Hanchang Shi ····· 1319

Photochemical degradation of nonylphenol in aqueous solution: The impact of pH and hydroxyl radical promoters
Aleksandr Dulov, Niina Dulova, Marina Trapido ····· 1326

A pilot-scale study of cryolite precipitation from high fluoride-containing wastewater in a reaction-separation integrated reactor
Ke Jiang, Kanggen Zhou, Youcai Yang, Hu Du ····· 1331

Atmospheric environment

Effect of phosphogypsum and dicyandiamide as additives on NH_3, N_2O and CH_4 emissions during composting
Yiming Luo, Guoxue Li, Wenhai Luo, Frank Schuchardt, Tao Jiang, Degang Xu ····· 1338

Evaluation of heavy metal contamination hazards in nuisance dust particles, in Kurdistan Province, western Iran
Reza Bashiri Khuzestani, Bubak Souri ····· 1346

Terrestrial environment

Utilizing surfactants to control the sorption, desorption, and biodegradation of phenanthrene in soil-water system
Haiwei Jin, Wenjun Zhou, Lizhong Zhu ····· 1355

Detoxifying PCDD/Fs and heavy metals in fly ash from medical waste incinerators with a DC double arc plasma torch
Xinchao Pan, Jianhua Yan, Zhengmiao Xie ····· 1362

Role of sorbent surface functionalities and microporosity in 2,2′,4,4′-tetrabromodiphenyl ether sorption onto biochars
Jia Xin, Ruilong Liu, Hubo Fan, Meilan Wang, Miao Li, Xiang Liu ····· 1368

Environmental biology

Systematic analysis of microfauna indicator values for treatment performance in a full-scale municipal wastewater treatment plant
Bo Hu, Rong Qi, Min Yang ····· 1379

Function of *arsATorf7orf8* of *Bacillus* sp. CDB3 in arsenic resistance
Wei Zheng, James Scifleet, Xuefei Yu, Tingbo Jiang, Ren Zhang ····· 1386

Enrichment, isolation and identification of sulfur-oxidizing bacteria from sulfide removing bioreactor
Jianfei Luo, Guoliang Tian, Weitie Lin ····· 1393

Environmental health and toxicology

In vitro immunotoxicity of untreated and treated urban wastewaters using various treatment processes to rainbow trout leucocytes
François Gagné, Marlène Fortier, Michel Fournier, Shirley-Anne Smyth ····· 1400
Using lysosomal membrane stability of haemocytes in *Ruditapes philippinarum* as a biomarker of cellular stress to assess contamination by caffeine, ibuprofen, carbamazepine and novobiocin
Gabriela V. Aguirre-Martínez, Sara Buratti, Elena Fabbri, Angel T. DelValls, M. Laura Martín-Díaz ····· 1408

Environmental catalysis and materials

Effect of transition metal doping under reducing calcination atmosphere on photocatalytic property of TiO_2 immobilized on SiO_2 beads
Rumi Chand, Eiko Obuchi, Katsumi Katoh, Hom Nath Luitel, Katsuyuki Nakano ····· 1419
A high activity of Ti/SnO_2-Sb electrode in the electrochemical degradation of 2,4-dichlorophenol in aqueous solution
Junfeng Niu, Dusmant Maharana, Jiale Xu, Zhen Chai, Yueping Bao ····· 1424
Effects of rhamnolipid biosurfactant JBR425 and synthetic surfactant Surfynol465 on the peroxidase-catalyzed oxidation of 2-naphthol
Ivanec-Goranina Rūta, Kulys Juozas ····· 1431

The 8th International Conference on Sustainable Water Environment

An novel identification method of the environmental risk sources for surface water pollution accidents in chemical industrial parks
Jianfeng Peng, Yonghui Song, Peng Yuan, Shuhu Xiao, Lu Han ····· 1441
Distribution and contamination status of chromium in surface sediments of northern Kaohsiung Harbor, Taiwan
Cheng-Di Dong, Chiu-Wen Chen, Chih-Feng Chen ····· 1450
Historical trends in the anthropogenic heavy metal levels in the tidal flat sediments of Lianyungang, China
Rui Zhang, Fan Zhang, Yingjun Ding, Jinrong Gao, Jing Chen, Li Zhou ····· 1458
Heterogeneous Fenton degradation of azo dyes catalyzed by modified polyacrylonitrile fiber Fe complexes: QSPR (quantitative structure peorperty relationship) study
Bing Li, Yongchun Dong, Zhizhong Ding ····· 1469
Rehabilitation and improvement of Guilin urban water environment: Function-oriented management
Yuansheng Pei, Hua Zuo, Zhaokun Luan, Sijia Gao ····· 1477
Adsorption of Mn^{2+} from aqueous solution using Fe and Mn oxide-coated sand
Chi-Chuan Kan, Mannie C Aganon, Cybelle Morales Futalan, Maria Lourdes P Dalida ····· 1483
Degradation kinetics and mechanism of trace nitrobenzene by granular activated carbon enhanced microwave/hydrogen peroxide system
Dina Tan, Honghu Zeng, Jie Liu, Xiaozhang Yu, Yanpeng Liang, Lanjing Lu ····· 1492

Serial parameter: CN 11-2629/X*1989*m*237*en*P*28*2013-7

Available online at www.sciencedirect.com
ScienceDirect
Journal of Environmental Sciences 2013, 25(7) 1368–1378
JOURNAL OF ENVIRONMENTAL SCIENCES
ISSN 1001-0742
CN 11-2629/X
www.jesc.ac.cn

Role of sorbent surface functionalities and microporosity in 2,2′,4,4′-tetrabromodiphenyl ether sorption onto biochars

Jia Xin, Ruilong Liu, Hubo Fan, Meilan Wang, Miao Li, Xiang Liu*

School of Environment, Tsinghua University, Beijing 100084, China. E-mail: xinj08@mails.tsinghua.edu.cn

Received 12 November 2012; revised 07 January 2013; accepted 24 January 2013

Abstract

The study provides insight into the combined effect of sorbent surface functionalities and microporosity on 2,2′,4,4′-tetrabromodiphenyl ether (BDE-47) sorption onto biochars. A series of biochars prepared under different conditions were used to test their sorption behaviors with BDE-47. The extents of sorption behaviors were parameterized in terms of the single-point adsorption equilibrium constant (K_{oc}) at three equilibrium concentration (C_e) levels ($0.001S_w$ (solubility), $0.005S_w$, and $0.05S_w$) which was determined using the Freundlich model. To elucidate the concentration-dependent dominant mechanisms for BDE-47 sorption onto biochars, K_{oc} was correlated with four major parameters using multiple parameter linear analysis accompanied with significance testing. The results indicated that at low concentration ($C_e = 0.001S_w$), the surface microporosity term, which represented a pore-filling mechanism, contributed significantly to this relationship, while as concentration was increased to higher levels, surface functionality related to surface adsorption began to take the dominant role, which was further confirmed by the results of Polanyi-based modeling. Given the above results, a dual mode model based on Dubinin-Radushkevich and de Boer-Zwikker equations was adopted to quantitatively assess the changes of significance of surface adsorption as well as that of pore filling with sorption process development. In addition, UV spectra of four typical aromatic compounds which represented the key structural fragments of biochars before and after interactions with BDE-47 were analyzed to determine the active functional groups and supply complementary evidence for the dominant interaction force for surface adsorption, based on which π–π electron-donor-acceptor interaction was proposed to contribute greatly to surface adsorption.

Key words: biochar; polybrominated diphenyl ethers (PBDEs); sorption; surface functionality; microporosity

DOI: 10.1016/S1001-0742(12)60222-8

Introduction

Polybrominated diphenyl ethers (PBDEs) are commonly used in industries due to their fire retarding properties, including in electrical appliances such as television and computers, building materials, and textiles (Alaee et al., 2003). They are a particularly problematic group of pollutants, not only because of their high level of toxicity at low concentrations but also because of their persistence in the environment and their tendency to bioaccumulation.

Recently, PBDEs were detected at high concentrations in various environmental compartments, of which soil was the most important phase for their accumulation and re-emission. Considerably high levels of PBDE congeners have been detected in soil samples from point source industrial areas, such as major e-waste recycling sites (Leung et al., 2007), PBDE production factory sites (Jin et al., 2011), and electronic appliance assembling sites (Zhang et al., 2009). In addition, PBDEs tend to be more and more widely detected in non-industrial areas, i.e., the Pearl River Delta (Guan et al., 2009), Yangtze River Delta (Duan et al., 2010), eastern urban area (Jiang et al., 2010) and central Loess Plateau (Meng et al., 2011), which may be caused by long-range transport and secondary emission. Thereby there is great urgency to control their further transport once PBDEs are released into the soil environment at high levels. Currently, "biochar," intentionally made by biomass pyrolysis, has received increasing attention as a possible soil amendment and a potential low-cost adsorbent to sequester contaminants and control pollutant migration (Zimmerman, 2010).

Like activated carbons, biochars are also produced by combustion processes (pyrolysis), but the source materials are generally limited to biological residues (e.g.,

* Corresponding author. E-mail: x.liu@tsinghua.edu.cn

wood, poultry litter, crop residues etc.) and not commonly activated or further treated before application to soils. Some biochars, unlike activated carbons, are not fully carbonized, and are therefore composed of different proportions of carbonized to amorphous organic matter and may react to contaminants in soils more like native soil organic matter (Beesley et al., 2011). Several previous studies have shown that the properties of biochars are strongly dependent on carbon precursor and formation conditions (Uchimiya et al., 2011; Wang et al., 2011), and that sorption properties are dependent not only on surface area and chemistry (Yu et al., 2010a; Zhang et al., 2011), but also on other properties, such as the char's content of authigenic organic phases (Yu et al., 2010b; Yan et al., 2011). As different mechanisms could impact the further fate and re-emission of sorbed contaminants after biochar amendments, to shed light on the involved mechanisms would pave a better way for post-remediation risk assessment and management.

Surface parameters and micropore structure are two classes of physicochemical properties that are recognized to exert an important influence on the extent of adsorption in biochar systems; they pertain to the coexisting interactions of surface adsorption and pore filling, respectively. The significance of surface adsorption or/and pore filling on hydrophobic organic compounds (HOCs) sorption has been pointed out in previous literature respectively (Zhu et al., 2005; Zhu and Pignatello, 2005a, 2005b; Ji et al., 2009). However, these previous works alluded to a single dominant sorption mechanism with little consideration given to the heterogeneous sorption development steps under specific conditions, so inconsistent and even contradictory conclusions have often been drawn about the contribution mode of simultaneously or separately involved surface adsorption and pore-filling mechanisms (Yang et al., 2006; Wang and Xing, 2007), which has created difficulties in clearly understanding the particular mechanism of interest and executing efficient related risk assessment.

In this study, batch sorption experiments were adopted to test the sorption behaviors of 12 biochars prepared from the same corn stalk at four pyrolytic temperatures (300°C, 400°C, 500°C, 600°C) with three different pyrolyzing periods (2, 4, 6 hr). Gradients of major physicochemical properties (such as O/C ratio, aromaticity, hydrophobicity and specific surface area (SSA)) were available among the prepared biochars. One typical PBDE congener, 2,2′,4,4′-tetrabromodiphenyl ether (BDE-47), which is included in the persistent organic pollutants (POPs) list and frequently detected in the natural environment at high concentration levels, was selected as the model PBDE to explore its interaction with the tested biochars. In order to attain deep insight into the coexisting interaction mechanisms of surface adsorption and pore filling, which depend on the sorption development process, the single-point sorption coefficient K_{oc} at three concentration levels (C_e (equilibrium concentration) = $0.001S_w$ (solubility), $C_e = 0.005S_w$, $C_e = 0.05S_w$) was respectively correlated with key physicochemical properties that were proposed to impact the sorption process using multiple linear regression analysis to determine the key molecular describer, accompanied with significance testing. Based on this analysis, a dual-mode model based on Dubinin-Radushkevich (DR) and de Boer-Zwikker equations was adopted to quantitatively assess the significance of surface adsorption as well as that of pore filling. In addition, according to the selected molecular describer for surface adsorption, the ultraviolet (UV) spectra of model aromatic compounds with similar aromatic backbone structure but different substituents before and after interaction with BDE-47 were obtained to determine the active sorption sites and functional group-related mechanism for surface adsorption.

1 Materials and methods

1.1 Chemicals

BDE-47 was purchased from Aldrich Chemical Co. Inc. (Milwaukee, USA) with a purity > 98%. BDE-47 has a $\log K_{ow}$ of 6.39, and solubility (S_w) of 94.7 μg/L. Stock solutions were prepared in methanol. Methanol and hexane were of high performance liquid chromatography (HPLC) grade (J. T. Baker, USA). All other chemicals ($CaCl_2$, NaN_3, HCl) were of analytical grade (Sinopharm Chemical Reagent Co., Ltd., China).

1.2 Preparation of biochars

Corn stalks (CS) were obtained from farmlands of the Daxing districts in Beijing and were used as received without pretreatments. Corn stalks were pyrolyzed at 300°C, 400°C, 500°C, and 600°C for 2, 4, 6 hr respectively under 1600 mL/min nitrogen flow rate using a box furnace (22 L void volume) with retort (Lindberg, Type 51662-HR, Watertown, WI, USA). The resulting biochars (CS300-2hr, CS400-2hr, CS500-2hr, CS600-2hr, CS300-4hr, CS400-4hr, CS500-4hr, CS600-4hr, CS300-6hr, CS400-6hr, CS500-6hr, CS600-6hr) were allowed to cool to room temperature overnight in the retort under 1600 mL/min nitrogen flow rate.

1.3 Characterization of biochar

Surface areas were measured in duplicate by nitrogen adsorption isotherms at 77 K using a NOVA 2000 surface area analyzer (Quantachrome, Boynton Beach, FL, USA). SSA was determined by the single-point method from adsorption isotherms with P/P_0 at 30%. Elemental composition (CHO) was determined by dry combustion using a Perkin-Elmer 2400 Series II CHNS/O Analyzer (Perkin-Elmer, Shelton, CT, USA).

To obtain information on surface functionalities, In-

frared spectra were obtained on a NEXUS 670 Fourier transform infrared (FT-IR) spectrometer (Thermo Nicolet Company, USA). The resolution of FT-IR was 4.0 cm^{-1}, and a total of 80 scans were collected for each spectrum.

The solid-state ^{13}C NMR spectra were obtained using cross-polarization (CP) and magic angle spinning (MAS) techniques. The NMR spectrometer was a Bruker DSX 400 MHz instrument (Bruker Co. Ltd., Germany), operating with CP (1 msec contact time) and MAS (5 kHz spinning rate) and a WB probe, at 75 MHz frequency for ^{13}C, with pulse width of 5 μsec, and 27 msec acquisition time. The rotor was 4 mm in diameter.

Surface functionalities, microporosity, aromaticity and hydrophobicity of the sorbents were indicated by the four major parameters O/C ratio, SSA, ($C_{\delta 108-162}$/ $C_{\delta 0-108}$) and (($C_{\delta 0-50}$ + $C_{\delta 108-162}$)/($C_{\delta 50-108}$ + $C_{\delta 162-220}$)) (based on ^{13}C NMR spectra, **Table S1**) respectively.

1.4 Sorption experiments

All sorption experiments were conducted in glass vials sealed with screw-caps to avoid evaporation loss. Each 1 mg sorbent sample was mixed with 40 mL of BDE-47 solution in 0.01 mol/L $CaCl_2$ as the background electrolyte and 0.2 g/L NaN_3 as a biocide with pH 7.0. The amount of sorbents added to the vials was controlled to achieve 20%–90% of solute uptake. Eight initial concentrations of BDE-47 in the range of 0.1–50 μg/L were prepared. Each concentration was prepared in triplicate, as well as blank samples without spiked BDE-47. Since a preliminary study had indicated that apparent equilibrium was achieved within 3 days (**Fig. S1**), the samples were shaken at 120 r/min at 25°C in the dark for 3 days. Then the glass vials were centrifuged for 20 min at 3000 r/min and the supernatants were withdrawn and analyzed by gas chromatography/mass spectrometry (GC-MS) for BDE-47. Details of the methodology for instrumental analysis can be found in the supplementary data.

Control reactors, prepared similarly but with no sorbent, were run in preliminary experiments to assess the loss of solute due to surface sorption and evaporation, and the results showed that average system losses were consistently less than 4% of the initial concentration for BDE-47, indicating that volatilization during sorption and uptake by the glass walls were negligible.

1.5 Analysis of UV spectra

Four typical aromatic compounds (phenol, diphenyl, benzoic acid, *p*-hydroxybenzoic acid) were employed as model compounds, which featured with the key structural fragments (aromatic backbone structure and different oxygen-containing substituents) of biochars, to explore the interaction mode between biochars and BDE-47. Taking benzoic acid for instance, for determination of UV spectra, benzoic acid working solutions were prepared at concentration of 200 mg/L in methanol and tagged as Group A. Then BDE-47 saturated solution was successively added to solutions of Group A to give a concentration of 20 mg/L, and these were tagged as Group B. BDE-47 solution of the same concentration without benzoic acid was used as spectral control. Each of the solutions of Group B was placed in a constant-temperature shaker for equilibrium for 30 min at 25°C. The UV spectra of the test solutions were recorded using a UV-Visible spectrophotometer (UV-1650PC, Shimadzu, Japan) against a solvent blank (for Group A) or BDE-47 blank (for Group B).

1.6 Data analysis

Two commonly applied isotherms were used, the organic carbon-normalized Freundlich Eq. (1) and the Dubinin-Astakhov (DA) equation for Polanyi-based modeling (Eq. (3)).

The Freundlich isotherm model has the following form:

$$q_{Foc} = K_{Foc} C_e^N \tag{1}$$

where, q_{Foc} (mg/kg) is the concentration on the solid phase normalized with F_{OC}, K_{Foc} ((mg/kg)/(μg/L)^N) is the Freundlich affinity coefficient, N is the isotherm linearity parameter, an indicator of site energy heterogeneity, and C_e (μg/L) is the liquid phase equilibrium concentration.

K_{oc} (L/g OC) is the single-point OC-normalized distribution coefficient (Eq. (2)).

$$K_{oc} = q_{Foc}/C_e \tag{2}$$

The Polanyi-based isotherm has the following form:

$$q_e = \rho_{sorbate} q'_{ad,max} \exp\left[-c\left[\frac{\varepsilon_{sorbate}}{n}\right]^d\right] \tag{3}$$

where, $\rho_{sorbate}$ (μg/L) is the assumed sorbate density based on neat chemical density at the temperature of interest, $q'_{ad,max}$ (mL sorbate/g sorbent) is the maximum adsorption capacity. c and d are empirical coefficients. $\varepsilon_{sorbate}$ (J/mol) is the adsorption potential, as expressed by Eq. (4):

$$\varepsilon_{sorbate} = R \times T \times \ln(S_w/C_e) \tag{4}$$

where, R is the gas constant, T is the Kelvin temperature. For weakly polar sorbates adsorbed on black carbon surfaces, the normalizing factor n can be usefully equated to:

$$n = V_s = \left(MW \times 10^6\right)/\rho_{sorbate} \tag{5}$$

where, V_s (μL/mol) is molar volume of the sorbate, and MW (μg/mol) is the molecular mass of the sorbate. The combined quantity ($\varepsilon_{sorbate}/n$, J/μL) is sometimes referred to as the adsorption potential density. c corrects for the use of V_s in normalizing sorption potential and d reflects the

nature of the stochastic distribution of $\varepsilon_{sorbate}/V_s$. In the work here, $q'_{ad,max}$, c, and d were fitted to the isotherm using the inverse of the observed q_e as a weighting coefficient.

q' is single-point sorption volume obtained as $q_e'/\rho_{sorbate}$.

The single-point OC-normalized distribution coefficients K_{oc} were then fitted using SPSS 17.0 and the following multiple linear equation:

$$K_{oc} = d_0 + d_1 \times \text{SSA} + d_2 \times (\text{O/C}) + d_3 \times (\text{aromaticity}) + d_4 \times (\text{hydrophobicity}) \quad (6)$$

where, d_0 is an intercept, d_1, d_2, d_3 and d_4 describe the dependence of the K_{oc} on SSA, O/C ratio, aromaticity and hydrophobicity.

As suggested by the statistical correlation results and Polanyi-based modeling results, sorption of BDE-47 onto biochars is ascribed to a combination of pore filling and surface adsorption. Therefore, a dual mode model (Eq. (7)), which combined the Dubinin-Radushkevich (DR) equation for describing a pore-filling process and de Boer-Zwikker equation describing a polarization-related surface adsorption process, was adopted to quantitatively assess of the contributions of pore-filling and surface adsorption mechanisms for BDE-47 sorption to three model biochars (CS400-4 hr, CS500-4hr, CS600-4hr), which were rich in micropores.

$$q_e = q_e^{por} + q_e^{sur} = q_{max}^{por} \times \exp\left[-\left(\frac{RTH}{\beta k}\right)^2 \ln^2\left(\frac{S_w}{C_e}\right)\right] + \frac{q_{max}^{sur}}{K_1}\left[\log\log\left(\frac{S_w}{C_e}\right) + K_2\right] \quad (7)$$

There are two terms q_e^{por} and q_e^{sur} in the equation, and q_e^{por} represents the pore-filling fraction of the sorbed amount described by the DR equation and q_e^{sur} represents the surface adsorption fraction of the sorbed amount described by the de Boer-Zwikker equation. H is the pore width. A more detailed description of the dual-mode sorption model is given in the supplementary data.

2 Results and discussion

2.1 Characterization of sorbents

Figure 1 provides the elemental ratio, BET-SSA, average pore diameter, aromaticity and hydrophobicity for biochar samples. Surface functionalities from FT-IR spectra, solid-state ^{13}C NMR spectra and integrated solid-state ^{13}C NMR data are supplied in **Figs. 2** and **3** and **Table S1**, respectively. Despite being from the same source material, the physicochemical parameters varied greatly among all the biochars prepared under different conditions (temperature and time specifically).

In terms of the temperature, with the same pyrolysis time, the increase of the pyrolysis temperature greatly impacted the parameters of the resulting biochars. Taking 4 hr for example, the H/C ratio dramatically declined in the order of 0.76 > 0.50 > 0.38 > 0.24 with the temperature increasing from 300 to 600°C, the diversity of functional groups indicated by FT-IR spectra was meanwhile negatively affected, and the adequacy of aromatic backbone structure was greatly enriched, all of which showed the process of carbonization was accelerated when the temperature was raised. In addition, the O/C ratio as a token of the polarity of the biochars gradually decreased in the order of 0.20 = 0.20 > 0.07 > 0.04, accompanied with the disappearance of bands of polar functional groups (O–H stretching (3200–3500 cm^{-1}), phenolic O–H stretching (1450 cm^{-1}), C–O–C stretching (1150 cm^{-1})) in the FT-IR spectra. Similar results were also obtained for a shorter-

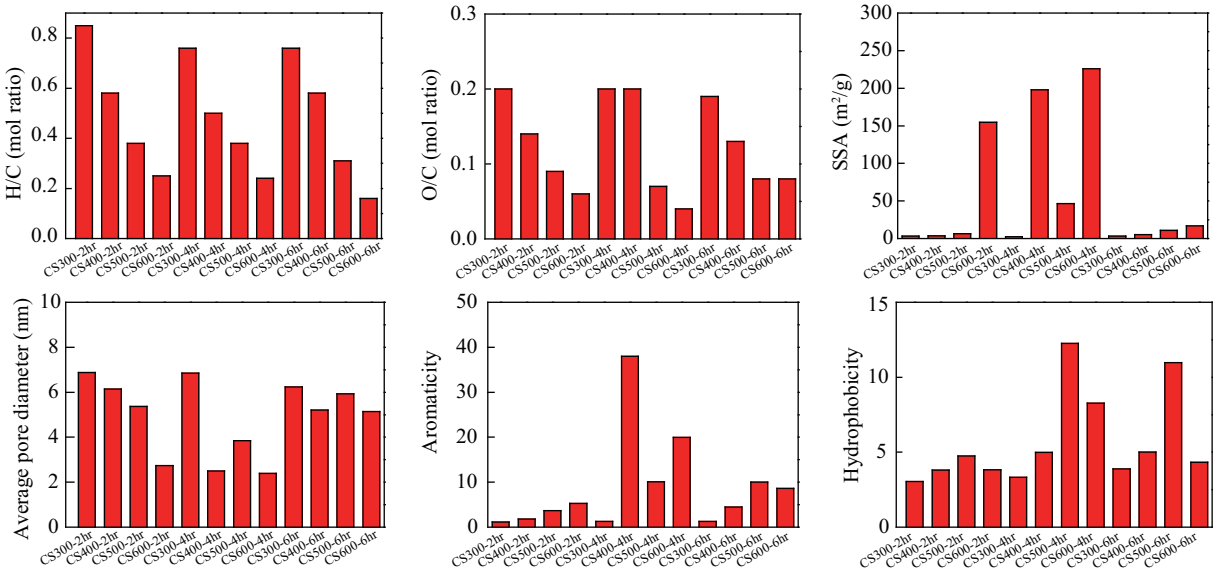

Fig. 1 Elemental ratio (H/C, O/C), SSA, average pore diameter, aromaticity and hydrophobicity for studied samples.

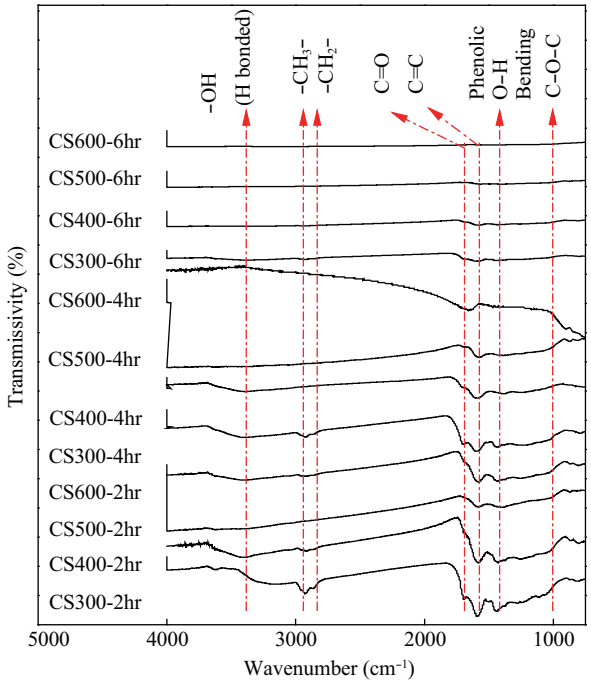

Fig. 2 FT-IR spectra of studied samples.

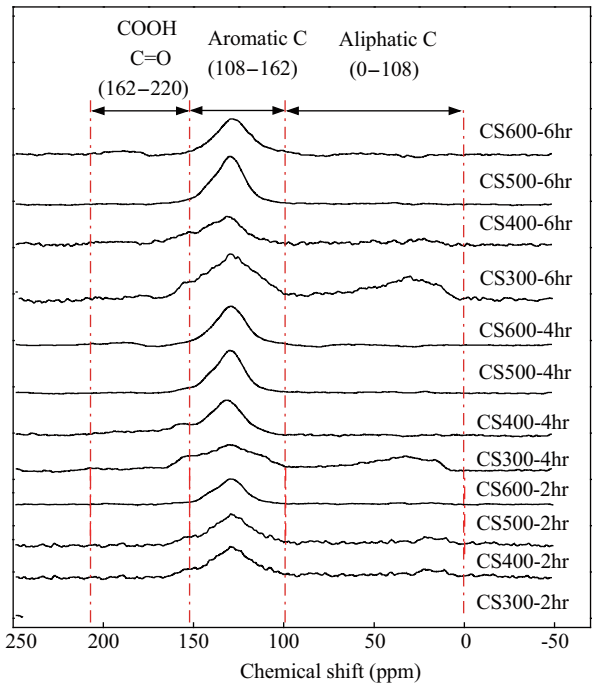

Fig. 3 ^{13}C NMR spectra of studied samples.

time case (2 hr) and longer-time case (6 hr). Moreover, it was observed that the higher temperature was favorable for the development of internal porous microstructures, which accounted for the huge SSA observed in CS400-4hr (197.85 m^2/g), CS500-4hr (46.29 m^2/g), CS600-4hr (225.87 m^2/g), yet absent from CS300-4hr (2.33 m^2/g).

In comparison with pyrolysis temperature, the effect of the pyrolysis time on surface properties of the resulting biochars was not very significant. For instance, fixed at 300°C, despite the prolonged pyrolysis time from 2 to 6 hr, no great differences in H/C ratios (0.85, 0.76, 0.76) were observed among three biochars (CS300-2hr, CS300-4hr, CS300-6hr) despite slight fluctuations of the values. Similar results were observed by comparing their FT-IR and ^{13}C NMR spectra. Yet in terms of internal microporous structures, they tended to be undermined as the pyrolysis process was prolonged, as a declined SSA was redisplayed in CS400-6hr after the full-fledged micropore structure was developed in CS400-4hr.

As for aromaticity and hydrophobicity (**Fig. 1**), both pyrolysis time and temperature exerted significant impact on the resulting biochar. The highest values of aromaticity and hydrophobicity were respectively obtained from CS400-4hr (37.99) and CS500-4hr (12.26). When the temperature and duration time further increased, a decreasing trend of aromaticity and hydrophobicity was observed.

2.2 Application of Freundlich isotherm and Polanyi-based isotherm

The Freundlich isotherm parameters are presented in **Table 1**. Great sorption affinity between BDE-47 and biochars was observed with high OC-normalized sorption coefficient K_{Foc}, which ranged from 180.78 to 1106.34 $(mg/kg)/(\mu g/L)^N$ for all the cases. Great disparity was observed between K_{Foc} values among the 12 biochar samples, which indicated that the organic carbon content and

Table 1 Carbon-normalized Freundlich coefficients K_{Foc} and Freundlich exponents (N) for studied samples

Sorbent	K_{Foc} $((mg/kg)/(\mu g/L)^N)$	N	R^2	K_{oc}		
				C_e/S_w = 0.001	C_e/S_w = 0.005	C_e/S_w = 0.05
CS300-2hr	726.77 ± 48.62	0.94 ± 0.06	0.991	837.17	760.11	662.03
CS400-2hr	436.95 ± 24.81	0.76 ± 0.03	0.997	769.32	522.82	300.85
CS500-2hr	190.64 ± 20.16	0.63 ± 0.04	0.992	460.31	252.14	106.57
CS600-2hr	345.00 ± 74.31	0.42 ± 0.09	0.898	1353.74	532.27	140.00
CS300-4hr	562.74 ± 100.98	0.87 ± 0.13	0.947	764.19	619.92	459.56
CS400-4hr	1106.34 ± 59.90	0.88 ± 0.07	0.985	1467.44	1209.72	917.67
CS500-4hr	362.76 ± 42.13	0.52 ± 0.05	0.978	1122.82	518.57	171.71
CS600-4hr	401.65 ± 80.87	0.44 ± 0.08	0.903	1501.03	580.35	167.37
CS300-6hr	569.49 ± 54.99	0.95 ± 0.08	0.987	640.72	591.18	526.89
CS400-6hr	392.86 ± 56.99	0.66 ± 0.07	0.978	863.86	504.40	233.60
CS500-6hr	180.78 ± 24.84	0.58 ± 0.05	0.986	486.50	247.47	94.084
CS600-6hr	493.83 ± 33.36	0.70 ± 0.04	0.993	1001.55	617.99	309.73

its related partitioning mechanism failed to play the only as well as the dominant role for BDE-47 sorption onto biochars at the concentration range 0.1–50 μg/L. In terms of *N* values, which represented the nonlinearity of the sorption isotherms, they varied a great deal (0.42–0.94) for the biochars that were prepared under different conditions.

In addition, the changes of sorption ability were concentration-dependent, which was shown by variations in single-point sorption coefficients K_{oc} calculated at three C_e levels ($C_e = 0.001S_w$, $C_e = 0.005S_w$, $C_e = 0.05S_w$). For instance, in comparison of the biochars (CS300-4hr, CS400-4hr, CS500-4hr, CS600-4hr) prepared under different temperatures yet for the same time span (4 hr), their K_{oc} values followed different orders at different equilibrium concentrations. At $C_e = 0.001S_w$, the K_{oc} values followed the order of CS400-4hr > CS500-4hr > CS600-4hr > CS300-4hr, while at $C_e = 0.05S_w$, the sequence became CS400-4hr > CS300-4hr > CS500-4hr > CS600-4hr, which was estimated to be ascribed to the changes of predominant sorption mechanisms. The *N* values, which were significantly lower than 1, also confirmed the co-existence of several involved mechanisms.

The DA formulation of the Polanyi-based isotherm approach explicitly considered the role of molar volume on adsorption capacity, while also explicitly attempting to account for the effects of temperature, solubility, and chemical size through its definition of adsorption potential density. In the case of all the biochars, fitted values of the exponent *d* showed *d*-values between 0.89 and 3.16 (**Table 2**). These results indicated heterogeneous distributions of adsorption potential domains, and suggested that some different sites were accessible to each group.

For the studied biochars, $q'_{ad,max}$ (0.96–55.82 mL/g) exceeded the values of micropore volume (**Table S2**), which implied substantial adsorption in macroporous regions and surface regions. We noted that the order of increasing sorption q' agreed precisely with the order of increasing C_e as shown in **Table 2**.

2.3 Correlation of sorption coefficients and biochar physicochemical properties (SSA and O/C ratio)

Multiple linear regression analysis was employed to explore the relationship between sorption capacity and biochar physicochemical parameters.

As indicated by the above results of Freundlich and Polanyi-based DA modeling, both surface adsorption and pore-filling mechanisms were involved within the sorption process between biochars and BDE-47. Different sorption behaviors shown by the K_{oc} under different concentration levels in this study indicated that the co-existing mechanisms contributed to the whole sorption process in a concentration-dependent way. In order to identify the contribution mode of various sorption mechanisms, the K_{oc} was correlated with various sorbent-specific parameters by multiple linear regression analysis accompanied with significance testing to determine the key molecular describer.

2.3.1 SSA

Results of analysis of the significance of the linear relationship as well as that of the parameters are shown in **Table 3**. At $C_e = 0.001S_w$, the *F*-test indicated that the correlation was statistically significant at a confidence level of 98.4%. The *t*-tests indicated that the SSA term contributed significantly to the relationship (at a confidence level higher than 96.9%). As reported in **Table 3**, the biochars showed a statistically significant ($P < 0.05$) positive dependence on SSA ($d_2 = 3.904$), indicating that K_{oc} increased with increasing SSAs. This suggested that pore filling should be the predominant mechanism for sorption at low concentration level ($C_e = 0.001S_w$). Yet at concentration $C_e = 0.005S_w$ and $C_e = 0.05S_w$, a poorly significant statistical correlation between the magnitude of sorption affinity and SSA variable was obtained, which showed that the importance and contribution of the pore-filling mechanism was weakened when the concentration increased.

The concentration-dependent importance of the pore-

Table 2 Fitted parameters of observed sorption data from Polanyi-based isotherms

Sorbent	$q'_{ad,max}$	*C*	*D*	R^2	q'		
					$C_e/S_w = 0.001$	$C_e/S_w = 0.005$	$C_e/S_w = 0.05$
CS300-2hr	2.28	11254.90	2.54	0.998	0.02	0.22	1.72
CS400-2hr	10.37	50.43	0.89	0.998	0.04	0.14	0.89
CS500-2hr	1.19	129.25	1.27	0.990	0.02	0.08	0.39
CS600-2hr	0.85	1389.40	1.98	0.960	0.02	0.10	0.54
CS300-4hr	14.68	167.39	1.20	0.947	0.02	0.13	1.63
CS400-4hr	55.82	86.76	0.99	0.985	0.05	0.29	3.29
CS500-4hr	1.00	1508.94	2.01	0.978	0.02	0.12	0.66
CS600-4hr	0.94	3217.24	2.22	0.968	0.02	0.12	0.68
CS300-6hr	5.46	599.89	1.62	0.995	0.02	0.14	1.60
CS400-6hr	4.04	63.92	1.01	0.984	0.04	0.13	0.68
CS500-6hr	0.96	126.30	1.28	0.996	0.02	0.08	0.35
CS600-6hr	1.08	74762.75	3.16	0.995	0.02	0.22	1.11

$q'_{ad,max}$ (mL sorbate/g sorbent) is the maximum adsorption capacity; *C* and *D* are empirical coefficients; q' is the single point adsorption capacity (mL sorbate/g sorbent) obtained as $q'_e/\rho_{sorbate}$.

Table 3 Multiple linear regression for the correlation between adsorption affinity coefficient and sample parameters

Concentration level	R^2	F-value	Confidence level forcorrelation significance		Significant?	
$C_e = 0.001S_w$	0.789	6.530	98.4%		Yes	
$C_e = 0.005S_w$	0.841	9.256	99.4%		Yes	
$C_e = 0.05S_w$	0.923	21.101	99.9%		Yes	
Concentration level	Parameter	Value	Standard error	t-Value	Confidence level for parameter significance	Significant?
$C_e = 0.001S_w$	O/C	152.424	1561.684	0.098	7.5%	No
	SSA	3.904	1.445	2.702	96.9%	Yes
	Aromaticity	–1.068	11.541	–0.093	7.1%	No
	Hydrophobicity	–3.654	29.425	–0.124	9.5%	No
$C_e = 0.005S_w$	O/C	2302.021	932.704	2.468	95.7%	Yes
	SSA	0.885	0.863	1.025	66.1%	No
	Aromaticity	11.044	6.893	1.602	84.7%	No
	Hydrophobicity	–14.398	17.574	–0.819	56.0%	No
$C_e = 0.05S_w$	O/C	3387.383	670.343	5.053	99.9%	Yes
	SSA	0.234	0.620	0.377	28.3%	No
	Aromaticity	9.762	4.954	1.971	91.1%	No
	Hydrophobicity	–10.131	12.631	–0.802	55.1%	No

filling mechanism was hypothesized in previous studies (Nguyen et al., 2007). Nguyen et al. (2007) supplied the evidence for pore filling by observing the order of increasing sorption, which agreed precisely with decreasing order of critical molecular diameter. However, in the same study, decreased effectiveness of pore filling for naphthalene and phenanthrene was also observed in that the $q'_{ad,max}$ calculated by Polanyi-based modeling exceeded the DFT or BJH estimate of combined micropore/mesopore volume, which implied substantial adsorption in the macroporous region and surface region.

Further evidence of the downshifting significance of the pore-filling mechanism and upshifting significance of surface adsorption was supplied by comparing the q' fitted with the Polanyi-based model and the micropore volume (**Table S2**). For instance, taking CS400-4hr which was rich in micropore structures for example, at $C_e = 0.001S_w$, its q' was 0.05 mL/g, which was smaller than its micropore volume (0.085 mL/g), indicating at least enough micropore sorption domains were available for its sorption. Nevertheless, as the equilibrium concentration increased to $C_e = 0.005S_w$ and $C_e = 0.05S_w$, the q' values were increased to 0.29 and 3.29 mL/g respectively, which were very much larger than their micropore volumes, indicating the involvement of other sorption mechanisms besides pore filling. Similar results were observed for all other biochars that were characterized with huge SSAs.

2.3.2 O/C ratio

The multiple linear regression results based on Eq. (8) are shown in **Table 3**. The O/C term exhibited marginal impact on the adsorption equilibrium constant when $C_e = 0.005S_w$. However, the t-tests showed that this term was significant when the concentration was increased to $C_e = 0.05S_w$, which indicated that the dominant role of the pore-filling mechanism was replaced by surface adsorption as the C_e gradually increased to a higher level (Chen et al., 2008). The result was corroborated by the above analysis of Polanyi-based model fitting results.

It has been reported that several mechanisms could contribute to surface adsorption, such as hydrophobic interactions, hydrogen bonding, π–π EDA interaction and Van der Waals' force (Cornelissen et al., 2005; Pan and Xing, 2008). As O/C would reflect the adequacy of both oxygen-containing functional groups and hydrophilic functional groups, its significant correlation with K_{oc} at higher C_e indicated that the dominant interaction strength must be closely related to O/C ratio, such as hydrophobicity, π–π EDA interaction, etc., thereby detailed analysis and extra auxiliary technologies should be combined for investigation of the specific sorption sites.

Significant contribution of π–π interactions to surface adsorption was proposed. Due to the strong electron-withdrawing ability of the ether group and Br group of BDE-47, the associated π-structures became electron deficient and thus acted as π-electron-acceptors to interact strongly with the π-electron-rich molecule surfaces (π-electron-donors) of the sorbents. Thereby π–π EDA interactions between BDE-47 and biochars may occur to dominate surface adsorption. In addition, the twisted configuration of the two ring moieties of BDE-47 provided a better access to biochar moieties as compared to polychlorinated and polybrominated biphenyls. This can enhance the π–π interactions and therefore impede desorption.

Previous studies have shown that π–π interactions were much stronger than van der Waals forces (Keiluweit and Kleber, 2009), thereby despite possible coexistence of

Table 4 Fitted parameters of observed sorption data by dual-mode model and specific contribution percentage of each fraction

Sample	DR fraction				de Boer-Zwikker fraction				R^2
	$\ln(q_{max}^{por})$	B	C_0 (μg/L)	Percentage (%)	$\frac{q_{max}^{sur}}{K_1}$	K_2	C_0 (μg/L)	Percentage (%)	
CS400-4hr	6.34 ± 0.33	1.057 ± 0.10	0.1	100.00	–6087.60 ± 119.52	–0.40 ± 0.01	0.1	0	
			5.0	66.29			5.0	33.71	0.989
			10.0	42.88			10.0	57.12	
			20.0	27.52			20.0	72.48	
			30.0	22.33			30.0	77.67	
			40.0	19.30			40.0	80.7	
			50.0	17.91			50.0	82.09	
CS500-4hr	5.63 ± 0.42	1.627 ± 0.05	0.1	100.00	–1714.43 ± 51.87	–0.39 ± 0.01	0.1	0	0.991
			5.0	60.29			5.0	39.71	
			10.0	34.81			10.0	65.19	
			20.0	29.53			20.0	70.47	
			30.0	26.08			30.0	73.92	
			40.0	23.72			40.0	76.28	
			50.0	22.86			50.0	77.14	
CS600-4hr	5.40 ± 0.51	1.041 ± 0.10	0.1	100.00	–1618.69 ± 101.52	–0.43 ± 0.03	0.1	0	0.878
			5.0	59.15			5.0	40.85	
			10.0	31.33			10.0	68.67	
			20.0	19.68			20.0	80.32	
			30.0	18.69			30.0	81.31	
			40.0	20.16			40.0	79.84	
			50.0	19.34			50.0	80.66	

hydrophobic interactions and π–π interactions, both of which benefited from hydrophilic functional groups, π–π interactions could overwhelm hydrophobic interactions to dominate the sorption process.

2.4 Quantitative assessment of the contributions of both pore filling and surface adsorption mechanisms with the dual mode model

As proposed above, pore filling and surface adsorption were both identified as two dominant mechanisms that were critical to the sorption process, and their contribution mode was impacted by the development of the sorption process. To better confirm the important role of both mechanisms and quantitatively assess their contribution mode, the DR model, which described the pore-filling-dominant sorption interaction, and the de Boer-Zwikker model, which reflected polarization-related surface adsorption, were effectively combined to quantitatively assess the changes in the dominant role of both mechanisms for micropore structured sorbents (CS400-4hr, CS500-4hr, CS600-4hr) as C_e increased.

The dual-mode model well described the sorption data for three porous biochars as shown in **Table 4** with good degree of fitting (R^2 = 0.989, 0.991, 0.878). The modeling result supplied further evidence for the two proposed dominant mechanisms: pore filling and surface adsorption. As shown in **Table 4**, taking CS400-4hr as an example, more and more sorption capacity (0–82.09%) was dominated by the surface sorption term, while the importance of pore filling (100%–17.91%) gradually declined as the initial concentration increased from 0.1 to 50 μg/L. Similar results were obtained for both other sorbents, CS500-4hr and CS600-4hr.

2.5 Analysis of surface interaction mechanism between BDE-47 and key oxygen-containing functional groups of biochars using UV spectroscopy

As the identification of key functional groups can supply more reliable evidence for the exploration of major sorption sites and the dominant surface interaction mechanism, the UV spectrum has often been used to study the intermolecular interactions owing to its high sensitivity. The absorbance of these aromatic compounds results from electronic transitions in the aromatic constituents, or chromophores, of these compounds. These transitions have been hypothesized to manifest themselves as maximum absorbance bands. The precise position, width, and intensity of these bands are strongly affected by substitution and conjugation of the chromophores. For instance, when π–π interaction was involved, the wavelength maximum of UV absorbance of the solution was found to be blue- or red-shifted to some extent in prior publications (He et al., 2008). In our study, four benzene derivatives (phenol, benzoic acid, *p*-hydroxybenzoic acid and diphenyl), which represented key structural fragments of biochars featured with similar aromatic structures but different substituents, were employed to study relationships between the changes in UV absorbance induced by charge complex formation, which made it immensely easier to follow the progress of π–π EDA reactions.

It can be observed from **Fig. 4** that an apparent red shift of the emission band from 222 to 228 nm occurred in the BDE-47 and phenol interaction process. For the

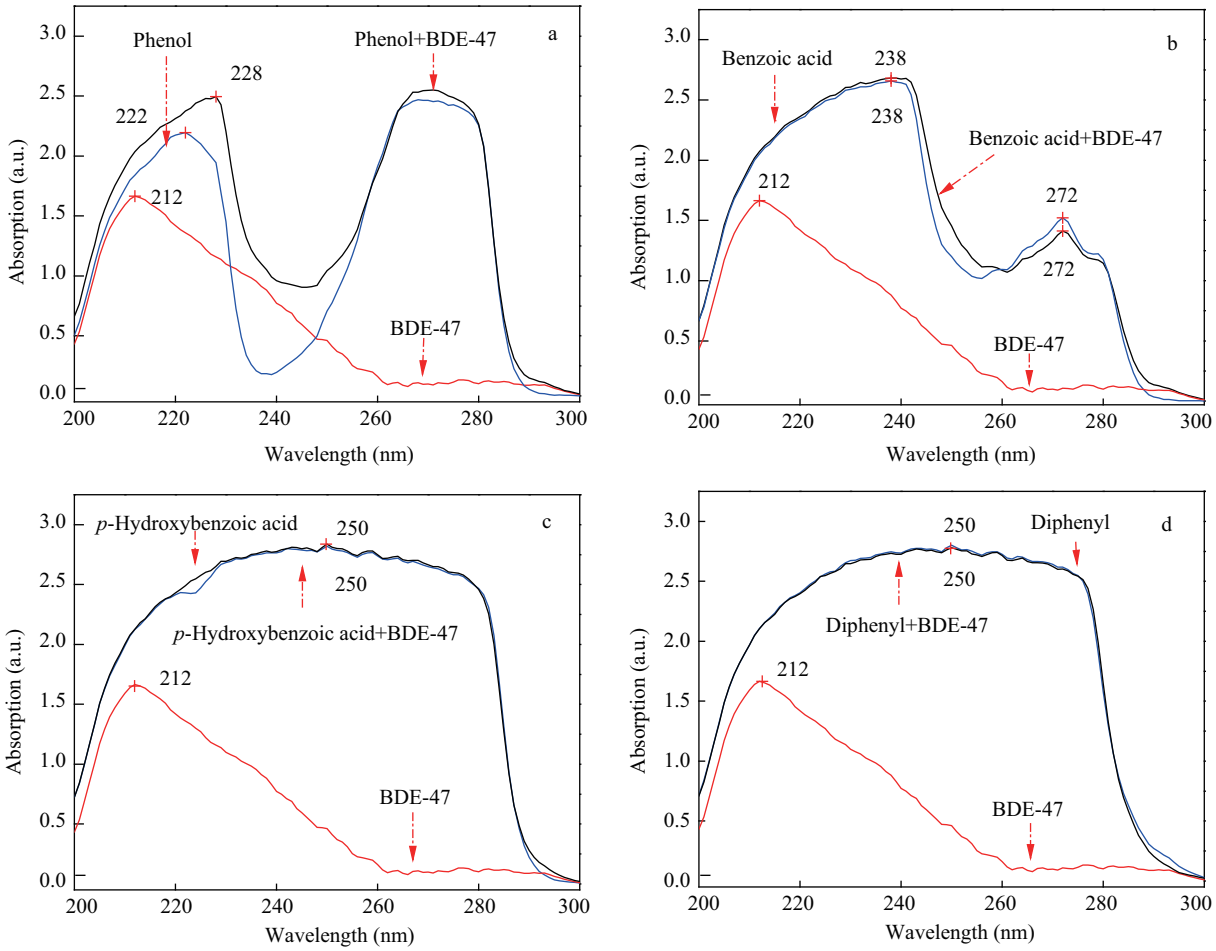

Fig. 4 UV spectra of model aromatic compounds (phenol (a), benzoic acid (b), *p*-hydroxylbenzoic acid (c), diphenyl (d)) before and after interaction with BDE-47.

case of benzoic acid, the absorption peaks of benzoic acid and BDE-47 were 238 and 212 nm, respectively, while with the addition of BDE-47 to the benzoic acid methanol solution, the maximum absorption spectra (λ_{max}) showed no significant change. Similarly, no significant changes of λ_{max} of UV absorption spectra were observed for *p*-hydroxybenzoic acid and diphenyl systems. The observable red shift for phenol has been attributed to complex formation between phenol and BDE-47 molecules through π–π EDA interaction.

The hydroxyl group (–OH) served as a good electron-donating substituent for aromatic rings, which helped to enhance the electron density of the ring and was conducive for occurrence of π–π interaction with the electron acceptor BDE-47. With the occurrence of π–π interaction, the electron density for phenol declined and resulted in the red shift of λ_{max} in the UV spectra.

Donor ability correlates with polarizability (Zhu et al., 2004), which increases with the number of rings in a fused-ring system, and the number and type of electron-donating substituents, such as alkyls. Acceptor ability is enhanced by electron-withdrawing substituents. The interactions of π-acceptor molecules with π-donating subunits are favored with increasing π-donating ability of the subunits. Biochars contained an abundance of potentially strong π-donor subunits, including aromatic rings substituted with two or more electron-donating groups such as hydroxyl and methoxyl groups. Therefore, the O/C ratio here greatly impacted the sorption process as a representative of polar aromatic substituents that contributed to enhance the π–π interaction strength.

In many previous studies, researchers attempted to discover a specific molecular descriptor which could be significantly correlated with the sorption abilities of the related sorbent, but with less dramatic results. In the review authored by Chefetz and Xing (2009), it was found that no significant correlations between either aromaticity or aliphaticity and sorption affinity were found for such a large and diverse data set. They suggested that neither aromaticity nor aliphaticity alone can be used to predict the sorption affinity of sorbents having wide and diverse properties; and they emphasized that polarity, with aromaticity or aliphaticity, might be used as a molecular parameter to evaluate sorption but only for chemically similar sorbents, which was in good agreement with our proposal of the significant role of O/C-related π–π EDA interaction.

3 Conclusions

In this study, based on a combination of statistical analysis, dual-mode model-based quantitative assessment and UV spectroscopy, the specific significance of pore filling as well as that of surface adsorption for biochars with various physicochemical properties was indentified. For biochars with developed micropore structures, with adequate sorption sites available and limited soluble sorbate molecules, pore filling tended to take effect significantly in the initial phase of sorption process and was gradually overwhelmed by surface adsorption. However, sorption on the biochars without developed internal micropore structure would greatly depend on their high polarity, especially functional groups which contributed to electron density change and π–π EDA interaction.

As land application of biochars gradually becomes an efficient and cost-effective contaminant sequestration strategy, the results in our study can supply theoretical evidence for risk assessment for biochar application to POP-contaminated site remediation according to the specific properties and qualities of the applied biochar. As the molecules sequestered within microporous biochars would be recalcitrant to short-term re-emission, this fraction of bound BDE-47 molecules was considered to be inert to chemical and biological reactions and less bioavailable, while for the fraction sorbed onto external surfaces, their re-emission would gradually occur despite a potentially large capacity for sorption.

Acknowledgments

This work was supported by the Special Environmental Research Funds for Public Welfare (No. 201209053).

Supporting materials

Supplementary data associated with this article can be found in the online version.

References

Alaee M, Arias P, Sjödin A, Bergman Å, 2003. An overview of commercially used brominated flame retardants, their applications, their use patterns in different countries/regions and possible modes of release. *Environment International*, 29(6): 683–689.

Beesley L, Moreno-Jiménez E, Gomez-Eyles J L, Harris E, Robinson B, Sizmur T, 2011. A review of biochars' potential role in the remediation, revegetation and restoration of contaminated soils. *Environmental Pollution*, 159(12): 3269–3282.

Chefetz B, Xing B S, 2009. Relative role of aliphatic and aromatic moieties as sorption domains for organic compounds: A review. *Environmental Science & Technology*, 43(6): 1680–1688.

Chen B L, Zhou D D, Zhu L Z, 2008. Transitional adsorption and partition of nonpolar and polar aromatic contaminants by biochars of pine needles with different pyrolytic temperatures. *Environmental Science & Technology*, 42(14): 5137–5143.

Cornelissen G, Gustafsson Ö, Bucheli T D, Jonker M T O, Koelmans A A, Van Noort P C M, 2005. Extensive sorption of organic compounds to black carbon, coal, and kerogen in sediments and soils: Mechanisms and consequences for distribution, bioaccumulation, and biodegradation. *Environmental Science & Technology*, 39(18): 6881–6895.

Duan Y P, Meng X Z, Yang C, Pan Z Y, Chen L, Yu R et al., 2010. Polybrominated diphenyl ethers in background surface soils from the Yangtze River Delta (YRD), China: occurrence, sources, and inventory. *Environmental Science and Pollution Research*, 17(4): 948–956.

Guan Y F, Sojinu O S S, Li S M, Zeng E Y, 2009. Fate of polybrominated diphenyl ethers in the environment of the Pearl River Estuary, South China. *Environmental Pollution*, 157(7): 2166–2172.

He Y Y, Wang X C, Fan X C, Zhao B, Jin P K, 2008. Interaction mechanism of anthracene with benzoic acid and its derivatives. *Chinese Journal of Chemistry*, 26(8): 1373–1379.

Ji L L, Chen W, Duan L, Zhu D Q, 2009. Mechanisms for strong adsorption of tetracycline to carbon nanotubes: A comparative study using activated carbon and graphite as adsorbents. *Environmental Science & Technology*, 43(7): 2322–2327.

Jiang Y F, Wang X T, Zhu K, Wu M H, Sheng G Y, Fu J M, 2010. Occurrence, compositional profiles and possible sources of polybrominated diphenyl ethers in urban soils of Shanghai, China. *Chemosphere*, 80(2): 131–136.

Jin J, Wang Y, Liu W Z, Yang C Q, Hu J C, Cui J, 2011. Polybrominated diphenyl ethers in atmosphere and soil of a production area in China: Levels and partitioning. *Journal of Environmental Sciences*, 23(3): 427–433.

Keiluweit M, Kleber M, 2009. Molecular-level interactions in soils and sediments: the role of aromatic π-systems. *Environmental Science & Technology*, 43(10): 3421–3429.

Leung A O W, Luksemburg W J, Wong A S, Wong M H, 2007. Spatial distribution of polybrominated diphenyl ethers and polychlorinated dibenzo-*p*-dioxins and dibenzofurans in soil and combusted residue at Guiyu, an electronic waste recycling site in southeast China. *Environmental Science & Technology*, 41(8): 2730–2737.

Meng X Z, Pan Z Y, Wu J J, Qiu Y L, Chen L, Li G M, 2011. Occurrence of polybrominated diphenyl ethers in soil from the central Loess Plateau, China: Role of regional range atmospheric transport. *Chemosphere*, 83(10): 1391–1397.

Nguyen T H, Cho H H, Poster D L, Ball W P, 2007. Evidence for a pore-filling mechanism in the adsorption of aromatic hydrocarbons to a natural wood char. *Environmental Science & Technology*, 41(4): 1212–1217.

Pan B, Xing B S, 2008. Adsorption mechanisms of organic chemicals on carbon nanotubes. *Environmental Science & Technology*, 42(24): 9005–9013.

Uchimiya M, Wartelle L H, Klasson K T, Fortier C A, Lima I M, 2011. Influence of pyrolysis temperature on biochar property and function as a heavy metal sorbent in soil. *Journal of Agricultural and Food Chemistry*, 59(6): 2501–2510.

Wang X L, Xing B S, 2007. Sorption of organic contaminants

by biopolymer-derived chars. *Environmental Science & Technology*, 41(24): 8342–8348.

Wang X S, Miao H H, He W, Shen H L, 2011. Competitive adsorption of Pb(II), Cu(II), and Cd(II) ions on wheat-residue derived black carbon. *Journal of Chemical and Engineering Data*, 56(3): 444–449.

Yan C X, Yang Y Y, Liu M H, Nie M H, Zhou J L, 2011. Phenanthrene sorption to Chinese coal: Importance of coal's geochemical properties. *Journal of Hazardous Materials*, 192(1): 86–92.

Yang K, Wang X L, Zhu L Z, Xing B S, 2006. Competitive sorption of pyrene, phenanthrene, and naphthalene on multiwalled carbon nanotubes. *Environmental Science & Technology*, 40(18): 5804–5810.

Yu X Y, Pan L G, Ying G G, Kookana R S, 2010a. Enhanced and irreversible sorption of pesticide pyrimethanil by soil amended with biochars. *Journal of Environmental Sciences*, 22(4): 615–620.

Yu X Y, Pan L G, Ying G G, Kookana R S, 2010b. Enhanced and irreversible sorption of pesticide pyrimethanil by soil amended with biochars. *Journal of Environmental Sciences*, 22(4): 615–620.

Zhang G X, Zhang Q, Sun K, Liu X T, Zheng W J, Zhao Y, 2011. Sorption of simazine to corn straw biochars prepared at different pyrolytic temperatures. *Environmental Pollution*, 159(10): 2594–2601.

Zhang X L, Luo X J, Chen S J, Wu J P, Mai B X, 2009. Spatial distribution and vertical profile of polybrominated diphenyl ethers, tetrabromobisphenol A, and decabromodiphenylethane in river sediment from an industrialized region of South China. *Environmental Pollution*, 157(6): 1917–1923.

Zhu D Q, Hyun S H, Pignatello J J, Lee L S, 2004. Evidence for π–π electron donor-acceptor interactions between π-donor aromatic compounds and π-acceptor sites in soil organic matter through pH effects on sorption. *Environmental Science & Technology*, 38(16): 4361–4368.

Zhu D Q, Kwon S, Pignatello J J, 2005. Adsorption of single-ring organic compounds to wood charcoals prepared under different thermochemical conditions. *Environmental Science & Technology*, 39(11): 3990–3998.

Zhu D Q, Pignatello J J, 2005a. Characterization of aromatic compound sorptive interactions with black carbon (charcoal) assisted by graphite as a model. *Environmental Science & Technology*, 39(7): 2033–2041.

Zhu D Q, Pignatello J J, 2005b. Characterization of aromatic compound sorptive interactions with black carbon (charcoal) assisted by graphite as a model. *Environmental Science & Technology*, 39(7): 2033–2041.

Zimmerman A R, 2010. Abiotic and microbial oxidation of laboratory-produced black carbon (biochar). *Environmental Science & Technology*, 44(4): 1295–1301.

Supporting materials

1 Supplemental details on instrument analysis methods

The determination of BDE-47 was performed using a 7890 gas chromatograph equipped with a 5975 MSD. The GC was operated in splitless injection mode. The carrier gas was He. A DB-5 MS chromatographic column (15 m × 0.25 mm (i.d.), and 0.1 μm (film thickness)) was used in a constant flow mode with the flow rate at 1.0 mL/min. The temperature rise program was: initial temperature at 140°C, held for 1 min, then increased to 170°C at the rate of 15°C/min and maintained for 1 min, and increased to 240°C at the rate of 8°C/min, and maintained for 1 min. Later, the temperature increased to 310°C at a rate of 35°C/min, and maintained for 4 min to remove the possible residual impurities. The MS was run under the electron impact ionization (EI) mode, in which the interface temperature was at 280°C, and the ionic source temperature at 250°C with electron energy of 70 eV, and the temperature of quadrupole at 150°C. The selective ion mode was utilized for the final quantification.

2 A dual mode adsorption model combining the Dubinin-Radushkevich (DR) equation and de Boer-Zwikker equation

2.1 DR equation

One of the most widely used isotherm equations in the characterization of pore structure and description of the micropore filling process in microporous adsorbents is the Dubinin-Radushkevich equation (Eq. (S1)) (Rodriguezreinoso et al., 2007). The Dubinin-Radushkevich (DR) equation has a uniform general form that is useful for most adsorbates and follows the expression Eq. (S1).

$$\theta = \frac{q}{q_{\max}} = \exp\left[-\left(\frac{A}{\beta E_0}\right)^2\right] \tag{S1}$$

where, θ is fractional adsorption, q is the amount adsorbed, $q_{\max}$ is the maximum capacity in the pore, whereas β and E_0 are an affinity coefficient and characteristic energy, respectively. The adsorption potential, A, when extended to liquid phase sorption (Tien, 1994) is usually expressed as Eq. (S2):

$$A = RT \ln\left(\frac{S_w}{C_e}\right) \tag{S2}$$

Here, R is gas constant and T is Kelvin temperature. S_w and C_e are the solute solubility and the equilibrium concentration respectively at given temperature T.

Theoretical studies of adsorption potentials between single molecules and model pores have shown that the characteristic energy, E_0, is a function of the microporous structure of the activated carbon, and this has been related empirically (Stoeckli 1977) to pore dimension by Eq. (S3):

$$E_0 = \frac{k}{H} \tag{S3}$$

where, k is a characteristic coefficient (≈24 kJ/(nm·mol)) and H is the width of pore.

Given to the above equations, the Dubinin-Radushkevich (DR) equation for liquid-soild sorption process can be expressed in the way:

$$q_e = q_{\max} \cdot \exp\left[-\left(\frac{RTH}{\beta k}\right)^2 \left(\ln\left(\frac{S_w}{C_e}\right)\right)^2\right] \tag{S4}$$

2.2 de Boer-Zwikker equation

Study of the previous literatures showed that isotherm equations have been derived by both de Boer and Zwikker (Hoover and Mellon, 1950) and Bradley for the assumed group which absorbs a first layer, and subsequent layers which are sorbed because of the dipole induced in the first layer. The equation is

$$\log\log\left(\frac{P}{P_0}\right) = \left(\frac{V}{V_m}\right)\log k_1 + \log k_2 \tag{S5}$$

In this equation, k_1 and k_2 are functions of the field of polar groups, the dipole moment of the sorbed gas, the polarizability of the gas and of the temperature. P and P_0 are equilibrium pressure and saturated vapor pressure of sorbed gas respectively. V and V_m are sorption capacity and saturated sorption capacity for monomolecular layer.

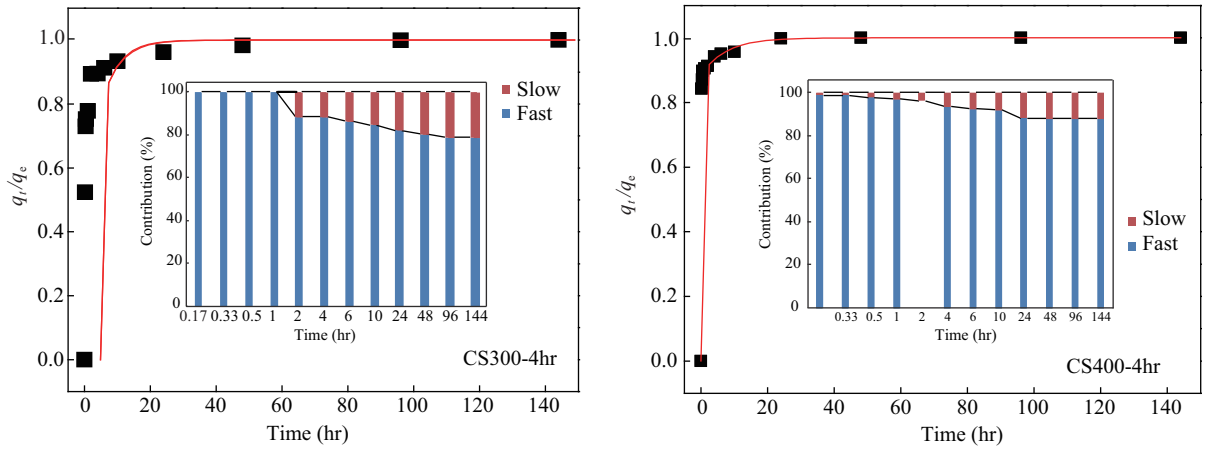

Fig. S1 Adsorption kinetic curves of BDE-47 onto CS300-4hr and CS400-4hr and the fitting results of by the two-compartment first-order model (solid line). The embedded plots exhibit the contributions of the fast sorption and the slow sorption to the total sorption capacities of BDE-47 at the different time intervals, respectively.

Table S1 Integration results of solid state ^{13}C NMR spectra and ratios of the aliphatic and aromatic peaks

Sample	0–50	50–60	60–96	96–108	108–145	145–162	162–190	190–220	Aliphatic C	Aromatic C
CS300-2hr	26.87	4.74	7.90	2.90	37.28	11.15	6.23	2.93	42.41	48.43
CS400-2hr	18.02	2.44	9.10	4.93	51.55	9.61	2.50	1.85	34.50	61.16
CS500-2hr	9.18	1.67	6.22	2.76	66.09	7.34	2.98	3.76	19.83	73.42
CS600-2hr	4.77	1.28	4.94	3.19	65.59	8.91	5.29	6.02	14.19	74.50
CS300-4hr	24.31	4.33	8.65	4.06	41.30	11.31	3.87	2.17	41.35	52.61
CS400-4hr	0.82	0.25	0.19	0.92	65.94	16.53	10.77	4.58	2.17	82.47
CS500-4hr	3.29	0.90	2.51	2.16	80.35	8.82	1.46	0.51	8.85	89.17
CS600-4hr	0.29	0.86	0.26	3.05	81.42	7.51	2.09	4.53	4.45	88.93
CS300-6hr	25.39	4.26	8.22	3.69	43.34	10.80	3.35	0.95	41.56	54.14
CS400-6hr	9.12	1.94	3.75	1.75	57.59	16.62	6.00	3.24	16.55	74.21
CS500-6hr	2.95	0.79	2.82	2.29	80.47	8.23	1.63	0.83	8.84	88.70
CS600-6hr	0.53	1.47	2.23	5.13	74.51	6.15	4.38	5.60	9.36	80.66

Table S2 Organic carbon (OC) content and pore size distribution for studied samples

Sorbent	OC (wt.%)[a]	V_t^b (cm^3/g)	V_{mic}^c (cm^3/g)	V_{mes}^d (cm^3/g)	V_{mic}/V_t
CS300-2hr	61.73	0.021	0.001	0.020	0.05
CS400-2hr	68.61	0.008	0.000	0.008	0
CS500-2hr	68.58	0.009	0.001	0.008	0.11
CS600-2hr	73.61	0.106	0.060	0.046	0.57
CS300-4hr	65.33	0.004	0.000	0.004	0
CS400-4hr	63.42	0.124	0.085	0.039	0.68
CS500-4hr	74.71	0.044	0.007	0.037	0.16
CS600-4hr	77.33	0.146	0.081	0.065	0.55
CS300-6hr	62.62	0.005	0.000	0.005	0
CS400-6hr	68.31	0.007	0.000	0.007	0
CS500-6hr	68.85	0.002	0.000	0.002	0
CS600-6hr	67.49	0.021	0.002	0.019	0.10

[a] Determined by elemental analysis; [b] total pore volume, determined at P/P_0 = 0.99; [c] micropore volume, calculated using the Horvath-Kawazoe method; [d] mesopore volume, calculated by V_t–V_{mic}.

Later the equation was used in liquid-soild interface system with the below expression:

$$q_e = \frac{q_{max}}{K_1}\left[\log\log(\frac{S_w}{C_e}) + K_2\right] \quad \text{(S6)}$$

In this equation, S_w and C_e are the solute solubility and the equilibrium concentration respectively, at given temperature T. q_e and q_{max} are the sorbed amount and maximum sorbed amount. K_1 and K_2 are functions of the field of polar groups, the dipole moment of the sorbate, the polarizability of the sorbate and of the temperature.

2.3 A dual mode isotherm by combining Dubinin-Radushkevich (DR) equation and de Boer-Zwikker equation

According to Eqs. (S4) and (S6), the dual mode isotherm can be described as:

$$q_e = q_e^{por} + q_e^{sur} = q_{max}^{por} \cdot \exp\left[-(\frac{RTH}{\beta k})^2 \ln^2(\frac{S_w}{C_e})\right] + \frac{q_{max}^{sur}}{K_1}\left[\log\log(\frac{S_w}{C_e}) + K_2\right] \tag{S7}$$

$$q_e = q_e^{por} + q_e^{sur} = q_{max}^{por} \cdot \exp\left[-(\frac{RTH}{\beta k})^2 \ln^2(\frac{S_w}{C_e})\right] + \frac{q_{max}^{sur}}{K_1}\left[\log\log(\frac{S_w}{C_e}) + K_2\right] \tag{S8}$$

There are two terms q_e^{por} and q_e^{sur} in the equation, and q_e^{por} represented pore filling fraction of sorbed amount described by DR equation and q_e^{sur} represented surface adsorption fraction of sorbed amount described by de Boer-Zwikker equation. q_{max}^{por} and q_{max}^{sur} represented the maximum sorption capacity of pore filling fraction and surface adsorption fraction respectively.

References

Hoover S R, Mellon E F, 1950. Application of polarization theory to sorption of water vapor by high polymers. *Journal of the American Society*, 72(6): 2562–2566

Rodriguezreinoso F, Garrido J, Martinmartinez J M, Molinasabio M, Torregrosa R, 1989. The combined use of different approaches in the characterization of microporous carbons. *Carbon*, 27(1): 23–32.

Stoeckli H F, 1977. Generalization of dubinin-radushkevich equation for filling of heterogeneous micropore systems. *Journal of Colloid and Interface Science*, 59(1): 184–185.

Tien C, 1994. Adsorption Calculations and Modeling. Butterworth-Heinemann Press, Boston.

JOURNAL OF ENVIRONMENTAL SCIENCES

环境科学学报(英文版)

(http://www.jesc.ac.cn)

Aims and scope

Journal of Environmental Sciences is an international academic journal supervised by Research Center for Eco-Environmental Sciences, Chinese Academy of Sciences. The journal publishes original, peer-reviewed innovative research and valuable findings in environmental sciences. The types of articles published are research article, critical review, rapid communications, and special issues.

The scope of the journal embraces the treatment processes for natural groundwater, municipal, agricultural and industrial water and wastewaters; physical and chemical methods for limitation of pollutants emission into the atmospheric environment; chemical and biological and phytoremediation of contaminated soil; fate and transport of pollutants in environments; toxicological effects of terrorist chemical release on the natural environment and human health; development of environmental catalysts and materials.

For subscription to electronic edition

Elsevier is responsible for subscription of the journal. Please subscribe to the journal via http://www.elsevier.com/locate/jes.

For subscription to print edition

China: Please contact the customer service, Science Press, 16 Donghuangchenggen North Street, Beijing 100717, China. Tel: +86-10-64017032; E-mail: journal@mail.sciencep.com, or the local post office throughout China (domestic postcode: 2-580).

Outside China: Please order the journal from the Elsevier Customer Service Department at the Regional Sales Office nearest you.

Submission declaration

Submission of an article implies that the work described has not been published previously (except in the form of an abstract or as part of a published lecture or academic thesis), that it is not under consideration for publication elsewhere. The submission should be approved by all authors and tacitly or explicitly by the responsible authorities where the work was carried out. If the manuscript accepted, it will not be published elsewhere in the same form, in English or in any other language, including electronically without the written consent of the copyright-holder.

Submission declaration

Submission of the work described has not been published previously (except in the form of an abstract or as part of a published lecture or academic thesis), that it is not under consideration for publication elsewhere. The publication should be approved by all authors and tacitly or explicitly by the responsible authorities where the work was carried out. If the manuscript accepted, it will not be published elsewhere in the same form, in English or in any other language, including electronically without the written consent of the copyright-holder.

Editorial

Authors should submit manuscript online at http://www.jesc.ac.cn. In case of queries, please contact editorial office, Tel: +86-10-62920553, E-mail: jesc@263.net, jesc@rcees.ac.cn. Instruction to authors is available at http://www.jesc.ac.cn.

Journal of Environmental Sciences (Established in 1989)

Vol. 25 No. 7 2013

Supervised by	Chinese Academy of Sciences	**Published by**	Science Press, Beijing, China
Sponsored by	Research Center for Eco-Environmental		Elsevier Limited, The Netherlands
	Sciences, Chinese Academy of Sciences	**Distributed by**	
Edited by	Editorial Office of Journal of	Domestic	Science Press, 16 Donghuangchenggen
	Environmental Sciences		North Street, Beijing 100717, China
	P. O. Box 2871, Beijing 100085, China		Local Post Offices through China
	Tel: 86-10-62920553; http://www.jesc.ac.cn	Foreign	Elsevier Limited
	E-mail: jesc@263.net, jesc@rcees.ac.cn		http://www.elsevier.com/locate/jes
Editor-in-chief	Hongxiao Tang	**Printed by**	Beijing Beilin Printing House, 100083, China

CN 11-2629/X **Domestic postcode: 2-580** **Domestic price per issue RMB ¥ 110.00**

ISSN 1001-0742